An Adaptive Fuzzy Mho Relay for Phase Backup Protection With Infeed From STATCOM

Sivaramakrishnan Raman, Ramakrishna Gokaraju, *Member, IEEE*, and Amit Jain, *Member, IEEE*

***Abstract*—This paper presents a fuzzy-logic-based scheme for the operation of generator-phase backup distance protection, otherwise popularly known as the "phase 21" function, in the presence of a STATCOM installed at the generator bus. The presence of STATCOM impacts the normal functioning of the distance relay based on its location as well as that of the fault. The method introduced here counters its adverse effects by formulating an adaptive mho relay for the phase 21 function, which accounts for the fast and dynamic compensation provided by the STATCOM throughout the operating time domain. Fuzzy logic is used in this paper to handle this varied compensation with its capability to process uncertain variation using linguistic variables to good effect. Two particular feature inputs from the STATCOM which have a direct impact on the reach of the relay are considered as the fuzzy system inputs. The objective is to counter and minimize the effect of current infeed from the STATCOM, on the apparent reach observed by the phase 21 relay and, thus, achieve the desired coordination. Electromagnetic transient simulations were used for the studies. The interaction between the simulation and the fuzzy system is performed online to further enable a closed-loop approach. Further furnished results validate the same interaction.**

***Index Terms*—Adaptive mho relay, fuzzy logic, generator phase 21 backup protection, STATCOM.**

I. Introduction

FLEXIBLE ac transmission systems (FACTS) devices have been a means to keep the power system stability margin safe and adequate. They, however, introduce operational concerns in power system protection with their fast dynamic nature being their attribute. The protection functions are based on an otherwise familiar or fixed network and are likely to malfunction if the device is not taken into account. A very interesting case pertains to distance protection wherein the apparent impedance seen by the relay undergoes a modification with the FACTS devices in place. The operation of distance relays being based on the impedance reach they observe at the given instant of time, requires accounting for the infeed or outfeed effects on the transmission line or the section they protect to perceive the true reach [1]–[3]. The presence of these devices within the fault loop may lead to maloperation in the form of relay underreach or overreach, more often than not. The fast acting and dynamic nature of the device makes the effect all the more transient and prevalent. The effects can percolate into the second zone of protection as well based on where the device is installed. This paper addresses this aspect using the scheme presented.

Of late, studies have been carried out for the sole purpose of investigating the effect of stationing a shunt FACTS device (STATCOM) on transmission protection applications. The work in [4] highlights that the distance relays employed for shunt-compensated lines tend to underreach, attributed to the fact that the R/X ratio of the line increases. In [5] and [6], a comparative study on the performance of distance relays protecting transmission lines compensated by shunt FACTS devices, namely, SVC and STATCOM with different faults, locations, and line lengths is considered. The authors show that STATCOM can result in overreaching as well if the system is weak and demanding even higher compensation. The study in [7] emphasizes the underreaching and overreaching effects in the presence of a simplified model of UPFC in the fault loop depending on its location. Investigations on similar lines are reported in [8] using a STATCOM. The relay reach problem studied in the literature available relates to only transmission-line protection. This paper, however, investigates the adverse impacts of placing a STATCOM within the reach of the generator phase backup distance function which has not been the focus so far. The phase 21 function [9]–[12] also employs a distance relay to protect the generator from uninterrupted fault current for prolonged periods. So the presence of any current infeed within the zonal reach of the relay should be taken into account [9], [13] since this function is set up to look into the system.

The relay reach problem in transmission-line distance protection has seen artificial neural networks (ANN) and support vector machines (SVMs) attempted as solutions for addressing it [14]–[16]. However, both methods tend to be basically trained classifiers or identifiers. They imitate a pattern observed in an existing set of inputs and the relation it holds with the output rather than use the natural understanding available from the system. An SVM-based technique was recently advocated in [14] to identify and discriminate the three zonal settings to achieve distance relay coordination on under various operating conditions pertaining to fault resistances, fault locations, and line flows. A stand-alone intelligent distance relay based on neural networks has been proposed in [15], wherein, the authors employ three ANNs to determine the correct trip boundaries of the distance relay in the presence of varying remote-end load or infeed with fault resistance. An ANN-based scheme was put forth [16] for the first zone protection accounting for the presence of the static synchronous series capacitor (SSSC) in the line.

Manuscript received October 10, 2011; revised April 06, 2012; accepted October 13, 2012. Date of publication December 13, 2012; date of current version December 19, 2012. Paper no. TPWRD-00863-2011.

S. Raman is with the University of Saskatchewan, Saskatoon, SK S7N 5A9 Canada. He is also with the International Institute of Information Technology, Hyderabad (IIIT H) 500 016, India (e-mail: sivaramakrishnan.raman@research.iiit.ac.in).

R. (Rama) Gokaraju is with the University of Saskatchewan, Saskatoon, SK S7N 5A9 Canada (e-mail: rama.krishna@mail.usask.ca).

A. Jain is with International Institute of Information Technology, Hyderabad (IIIT H) 500 016, India (e-mail: amit@iiit.ac.in).

Digital Object Identifier 10.1109/TPWRD.2012.2226062

Fuzzy logic, on the other hand, uses a rule base with the inputs expressed in the form of linguistic variables. The method is thus capable of finding the relay reach in a natural and accurate fashion. The use of fuzzy logic to address the relay reach problem due to FACTS device placement has never been reported so far for distance protection. More important, it has never been done for the phase 21 function. Fuzzy-logic-related work has so far catered to only transmission-line distance protection. Further, it has been only to issue the correct trip signal for different kinds of faults as in [17] and [18] and not to address the specific problem of relay reach from infeed. This paper proposes a different approach with the application of fuzzy logic to mitigate the transient interference owing to STATCOM infeed in the "Phase 21" function. It develops a relaying procedure centered on an adaptive mho circle. Two main contributions this paper come forward, which are: 1) addressing the relay reach problem in the generator phase 21 function while the existing literature focuses on the same problem only in transmission-side protection and 2) application of the fuzzy logic's capability of handling the uncertain variation in STATCOM variation, which has not been attempted so far.

This paper discusses the basis of phase 21 protection, followed by an illustration of the STATCOM infeed effect on the system, in Section II. Section III details the system specifics of the transient simulation model. Section IV introduces fuzzy logic before elaborating on the fuzzy scheme implementation. Section V provides various results and discusses relevant issues, such as current-transformer (CT) saturation, breaker operation, and consideration of the generator capability curve (GCC).

II. Phase 21 Backup and STATCOM Effect

A. Generator-Phase Backup

The generator-phase backup facility [9], [10] is present to prevent damage to the equipment when a fault in the system external to the generator does not get cleared by the primary protection, local breaker failure schemes, or even the backup protection functions in the transmission system. A specified delay is instituted in the relay operation for it to coordinate with every other relay that is supposed to operate beforehand. The phase 21 backup function is designed to work specifically for phase-to-phase faults alone and does not cater to ground faults which are taken care of by a different arrangement, such as voltage-restrained overcurrent relays. Fig. 1 shows an arrangement of the phase 21 setup for a synchronous generator connected to a system. The phase 21 function can also look into the faults in the generator [10], [12], but this particular setup shows that only faults external and looking into the system are identified by this phase 21 function. Generally, the relay makes use of two mho zones. However, when only one zone is to be used, the second zone setting is adopted from one of the following principles outlined by the Power System Relaying Committee [9]:

1) 120% of the longest line from the generator;
2) 50%–67% of the generator load impedance at the rated power factor angle (RPFA); in other words, 150%–200% of generator rated meghavolt-amperes is covered;

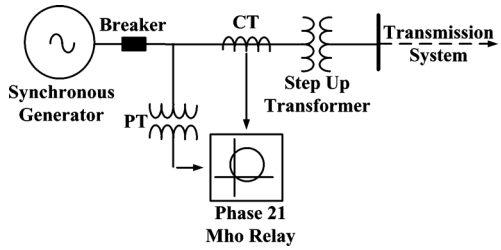

Fig. 1. Generator Phase 21 relay setup.

3) 80%–90% of the generator load impedance at the maximum torque angle (MTA), which is generally specified at about 85%.

The zone II reach is chosen as the only mho zone for the phase 21 relay. Thus, it is better that the longer reach take the generator load into account. This paper makes use of the setting (ii) specified before. If the system in Fig. 1 was radial, the problem regarding the load impedance does not arise [12]. However, when the system is fed from more than one terminal, it is necessary to take it into consideration. The generator capability curves in the P-Q plane can be transferred onto the R-X plane. The mathematical description for the phase 21 reach [9] is given in

$$|Z_G| = \frac{kV_g^2}{\mathrm{MVA}_G}\left(\frac{R_c}{R_v}\right)$$
$$Z_{reach} = \frac{|Z_G|^* 0.67}{\cos(\mathrm{MTA} - \mathrm{RPFA})}\angle \mathrm{MTA} \quad (1)$$

$|Z_G|$ is the generator load impedance magnitude, and kV_G and MVA_G are the rated kilovolts and megavolt-amperes of the synchronous generator. R_c and R_v denote the current and voltage transformer ratio, respectively. It is general practice to allow for 150%–200% of loading. In other words, it is 0.67 to 0.5 times the value of $|Z_G|$. MTA is the maximum torque angle set generally at about 85° and RPFA is the rated power factor angle in the system.

B. Effect of the Infeed From STATCOM

A simpler system has been considered in Fig. 2 to highlight the effect of current infeeds on the zonal reach of distance relays [1]–[3]. Zone I of relay AB protects only 80% of the line and, thus, measures fault current directly. If the same relay is to protect the complete adjoining section BC in a delayed zone of operation, it measures a current quite different from the fault current at F. The fault current has contributions in remote branches from buses D and E, resulting in current infeed. The relay thus no more observes the correct apparent impedance. It is evident on the basis of simple Kirchhoff's Law equations in (2)–(4) that the relay would have an incorrect reach setting if it is fixed at $(Z_{AB} + Z_{BC})$

$$I_{BF} = I_{\mathrm{relay}} + I_{DB} + I_{EB} \quad (2)$$
$$V_{\mathrm{relay}} = I_{\mathrm{relay}} Z_{AB} + I_{BF} Z_{BF} \quad (3)$$
$$Z_{new} = \frac{V_{\mathrm{relay}}}{I_{\mathrm{relay}}} = Z_{AB} + \frac{I_{BF}}{I_{\mathrm{relay}}} Z_{BF} \quad (4)$$

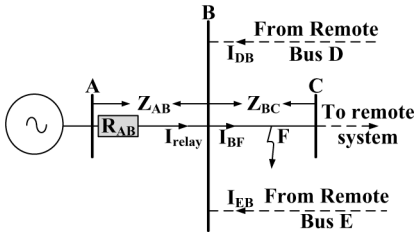

Fig. 2. Illustration of the current infeed effect.

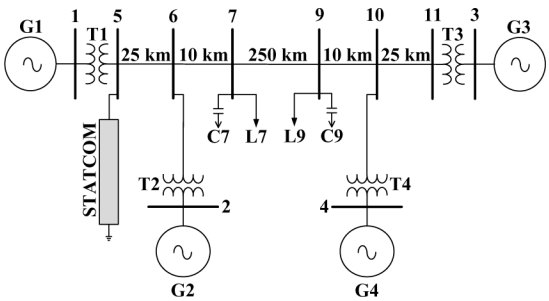

Fig. 3. Single-line diagram of the system used for simulation.

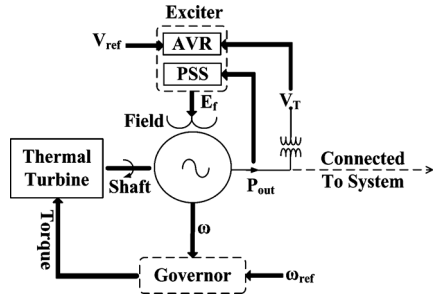

Fig. 4. Synchronous generator model.

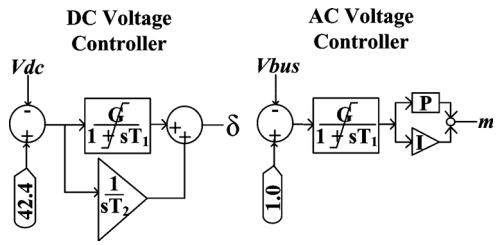

Fig. 5. STATCOM ac and dc controllers.

where Z_{AB}, Z_{BC}, and Z_{BF} are the corresponding line or section impedances.

The model in Fig. 3 with the synchronous generator and STATCOM is a transient one as a result of which the current contributions are no more steady-state values. To calculate the reach by (4), the computation is to be carried out every simulation step as the STATCOM imports or exports reactive power in a dynamic fashion to keep up with the demand. This paper uses an alternative method which also measures every time step but instead calls upon the fuzzy logic's capability to address the transiently varying infeed. The phase 21 relay in Fig. 1 covers a reach as per the norm given in point (ii) in the previous section. This easily spans the stepup transformer's impedance and the transmission line beyond the STATCOM in Fig. 3 which makes the model suitable for testing this application if there is a fault on the transmission side.

III. Simulation System

Fig. 3 shows the one-line diagram of the system modeled using an electromagnetic transient program environment [19]. The specifications of the system are given in Appendix A. The model uses a 4-generator system [20] spanning two areas connected by a transmission line 250 km long between buses 7 and 9. The line is series compensated with a capacitor, and the end buses are provided with shunt capacitors and loads. The STATCOM is stationed at bus 5 to provide reactive power support to G1.

The synchronous generator model used is a thermal/steam generator, the ratings and specifications of which are listed in Appendix A. The exciter and turbine/generator models are interfaced directly with the synchronous machine model as shown in Fig. 4. The exciter model in place here is a standard IEEE ST1A-type static exciter [21]. The power system stabilizer (PSS) was designed using a lead lag-based controller [21] whose gain and time constant parameters have been tuned on lines similar to [22].

A. STATCOM Model

The STATCOM model used in the simulation employs the working principle of a two-level, three-phase, six-pulse voltage-source converter (VSC) [23]. The stiff dc voltage to be provided to the ac system is fed by a capacitor serving as a dc link. The STATCOM is interfaced with the system through a coupling transformer. The specifics of the components are given in Appendix B. The steady-state control logics for the STATCOM unit are depicted in Fig. 5. It consists of an ac as well as dc control loop constituting proportional-integral controllers. They are set to control the ac bus voltage *Vbus* on the reference value fixed at 1 p.u. and capacitor or dc-link voltage *Vdc* on the reference value fixed at 42.4 kV. The control parameter values are given in Appendix B. If the reference value of 1 p.u. is greater than the voltage *Vbus*, the control action injects reactive power from the converter to the system (capacitive action). However, if the bus voltage *Vbus* is greater than the reference, the reverse (inductive action) is prompted [23].

The firing sequence of the gate turn off (GTO) thyristors is controlled by the pulsewidth modulation scheme shown in Fig. 6. It works on the frequent crossover between a sinusoidal modulating (reference) signal and a triangular carrier signal which has a frequency many times that of the modulating signal. The modulating signal has the fundamental frequency. The width of the triggering gate turn on and turn off pulses is controlled by the ratio of the amplitudes of the modulating and carrier signals, known as the modulation index m. The value m eventually also controls the fundamental magnitude of the ac signal *Vac* produced by the converter. In order to maintain a constant dc voltage *Vdc* at the capacitor, a voluntary phase shift between the bus voltage *Vbus* and *Vac*, known as the phase-shift order δ is introduced. This actually leads to the transfer of a small amount of active power which accounts for the losses in the converter switches [23]. Thus, the ac controller yields m while the dc controller yields δ as outputs.

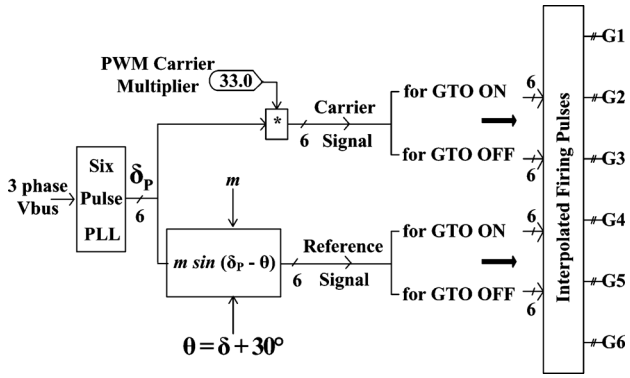

Fig. 6. Six-pulse GTO firing circuit.

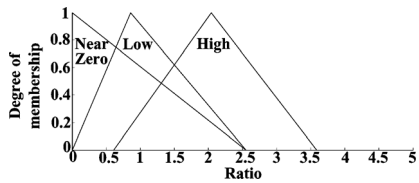

Fig. 7. Membership functions for feature 1.

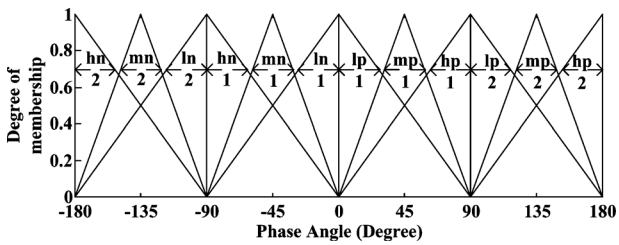

Fig. 8. Membership functions for feature 2.

IV. Proposed Fuzzy-Logic-Based Scheme

A. Preprocessing of Inputs and Fuzzification

The proposed method uses two feature variables of STATCOM taken as measurements from the simulation to act as fuzzy system inputs. They have a considerable relation with the infeed and its effect on the reach. The two quantities are: a) the "ratio" of the infeed current and relay current magnitudes and b) "phase-angle difference" between the two. These quantities are accessed from the simulation itself at every time step by designing a few computational blocks. This is done for each kind of relay. Because only phase relays are included, there are three relays each of which requires these two quantities. The currents measured are of the form I_{p1}–I_{p2} for the phase relay concerning phases $p1$ and $p2$. The magnitude, phase angle, and sequence components are computed using a fast Fourier transform (FFT) block in PSCAD/EMTDC. The inputs thus obtained are fuzzified using triangular membership functions shown in Figs. 7 and 8.

The first input, ratio, has three membership functions characterized by the linguistic variables: near-zero, low, and high. The second input, phase angle, has 12 membership functions resulting from two for each linguistic variable: low positive (lp1 and lp2), medium positive (mp1 and mp2), high positive (hp1 and hp2), low negative (ln 1 and ln 2), medium negative (mp1 and mp2), and high negative (hn1 and hn2). The "1" refers to the quadrant from 0°–90°, while "2" refers to the quadrant from 90°–180° for positive, medium, and negative functions. The functions range over −180° to 180° covering a complete 360° cycle.

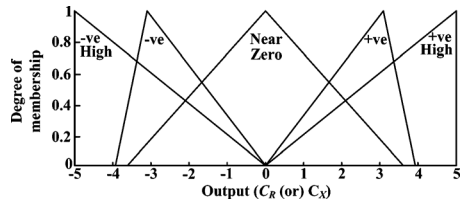

Fig. 9. Membership function for the two outputs.

B. Fuzzy Inference Engine: Rule Base and Defuzzified Output

The fuzzy inference system (FIS) in use here is of the "Mamdani" type [24].

1) Rule Implication: A set of 25 independent rules has been framed based on known facts to apply toward the inputs obtained from the simulation. The extent to which a rule is fired is decided by using the max or min operator [24].

2) Aggregation: The outputs used in this scheme are percentage factors by which the x and y coordinates of the relay reach are modified. There are two outputs C_R and C_X, having five membership functions each, named after the linguistic variables: very negative, negative, near zero, positive, and very positive. However both are identical to the one shown in Fig. 9. The degree by which a rule is fired also determines the area of the output membership function. The final conjoined output surface obtained from the max aggregation method is defuzzified into a single crisp value using the centroid defuzzification method [24].

C. Postprocessing—Online Closed-Loop Simulation

Once the defuzzified or crisp value of C_R and C_X are obtained for a simulation step, they should be made use of in the same simulation to serve the objective. The two outputs are used as a percentage increase (for positive output) and percentage decrease (for negative input) in the relay reach. However, it is important to note that only the reach beyond the point of infeed is affected. Thus, the factor computed from the fuzzy inference system is applied only to that particular reach, keeping the other part intact. If resistive and reactive reach beyond infeed is originally fixed at $R2$ and $X2$, (5) gives new reach beyond infeed

$$\begin{aligned} R2_{new} &= R2(1 + C_R) \\ X2_{\text{new}} &= X2(1 + C_X). \end{aligned} \tag{5}$$

The total reach is derived by adding what is obtained in (5) to the transformer impedance given by $X1$ which is the impedance behind the infeed.

1) Closed-Loop Linkage: The electromagnetic transient simulation is made capable of calling the fuzzy algorithm for the adaptive relay from within its environment to ensure it is online as shown in Fig. 10.

With the breakers operating on the signals from the relays, it can be regarded a closed-loop experiment. It is not technically

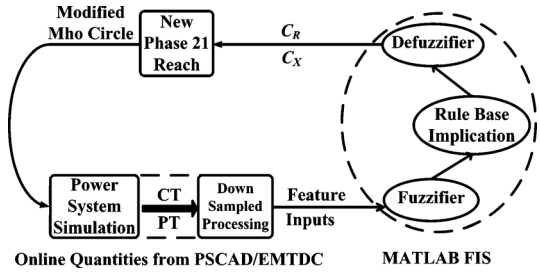

Fig. 10. Scheme of the proposed closed-loop method.

feasible to apply the routine specified for every simulation time step (25 μs). To address this, a downsampling logic is used to employ the fuzzy-logic scheme at specific intervals.

D. Fuzzy Membership Training

It is important that the mathematical functions defining the memberships are tuned suitably to the needs of the problem. A set of inputs and correspondingly known outputs forms the training set. The inputs are given by various sets of values corresponding to the ratio and phase-angle differences. The outputs are the expected values for the new reach of the relay. The set of inputs and outputs can be extracted from the simulation itself in huge numbers as is the case generally. However, in order to avoid the training from being simulation specific, the set of inputs has been generated on a random basis in large numbers (500–1000) and the expected values are calculated on the basis of (4). A "Constrained Non-linear Optimization" for minimizing the objective function (6) subject to various constraints is thus developed

$$J = \sum_i \left[(r_i - f1_i)^2 + (x_i - f2_i)^2 \right] \tag{6}$$

where r_i and x_i are the expected modified reaches for random set i; and $f1_i$ and $f2_i$ are the corresponding values obtained from the FIS. The nonlinear optimization routine is performed to tune the fuzzy membership functions. Once tuned, the same memberships are used in the online procedure given in section C. Figs. 7–9 actually represent the tuned values of the functions obtained from the nonlinear optimization.

V. Simulation Studies

A. Modeling

The four-generator system shown in Fig. 3 has been modeled using an electromagnetic transient simulation in PSCAD/EMTDC. The STATCOM device is located between the generator stepup (GSU) transformer and the adjoining bus looking into the system. The faults considered are simulated in the middle of the transmission-line section between buses 5 and 6 (25 km) as it is aptly located immediately beyond the GSU transformer and the STATCOM. This line is modeled as a pi section model, the parameters of which are given in Appendix A. Equation (1) moreover would cover both the GSU and the 25-km line. If the fault is beyond the location of the STATCOM as is the case chosen, the simulation shows the

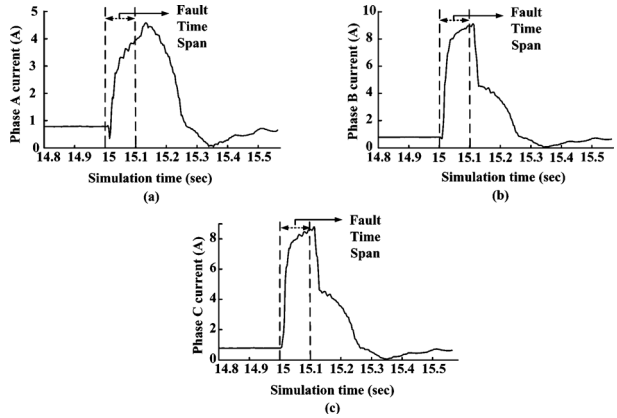

Fig. 11. STATCOM infeed current magnitude for phase fault BC, as seen by the CT secondary in (a) phase A, (b) phase B, and (c) phase C.

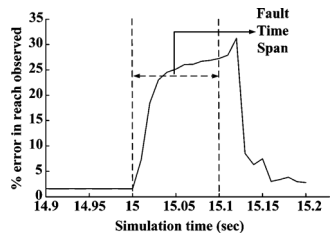

Fig. 12. Percentage error of observed reach against true reach.

impact of the infeed. All phase faults not involving ground are first studied in depth (A-B, B-C, and C-A).

B. Effect of STATCOM Infeed

A measure of how much compensation is provided by the STATCOM would help study the effect of STATCOM on the relay reach. Fig. 11 depicts the STATCOM current magnitudes in each of the three phases for a phase-to-phase B-C fault. The currents, given in amperes, are those at the secondary of the CTs used to measure them. The fault is applied at the simulation time equal to 15 s for the duration of 0.1 s. It shows no considerable contribution in the time before the fault occurs. Once the fault is cleared, it reduces drastically. However, when the fault occurs, the STATCOM delivers a good amount of compensation and this is where the relay reach affected the maximum. Hence, the STATCOM effect is more visible when the relay is required to function.

Further evidence of STATCOM infeed can be seen from Fig. 12 which plots the percentage error in relay reach observed by relay BC for BC fault, against the true reach as the reference value. The true reach is the reach that should be observed ideally by the relay if the infeed is accounted for. It is calculated based on (4) for the sake of comparison. It can be noted that the percentage error is the maximum in the fault duration.

C. Performance of the Fuzzy-Logic-Based Mho Relay

The method described in Section IV is applied here. The fuzzy memberships are tuned as explained before and the resulting functions are those shown in Figs. 7–9. The relay uses only a single mho zone. The reach covers the generator stepup transformer, and the entire length of the 25-km line out of the

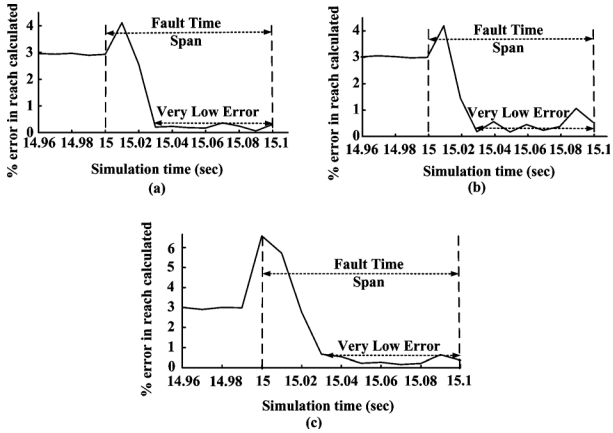

Fig. 13. Percentage error in calculated reach of (a) relay AB for fault A-B, (b) relay BC for fault B-C, and (c) relay CA for fault C-A. The fault initiation time = 15 s.

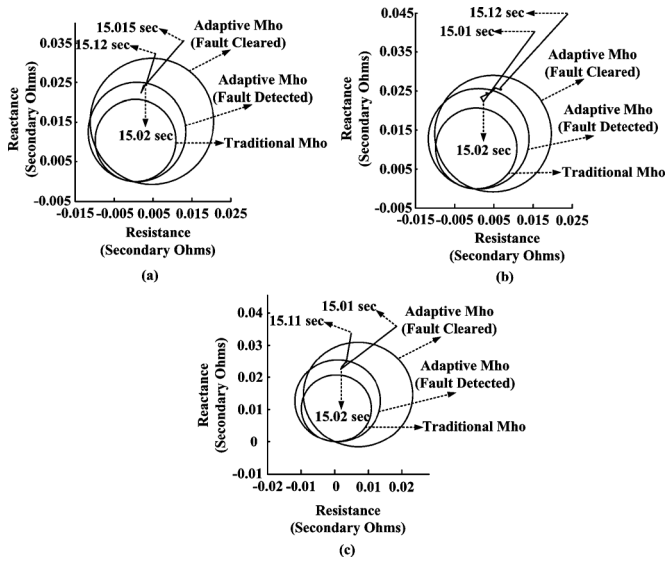

Fig. 14. Fuzzy adaptive mho zonal descriptions of (a) relay AB for the A-B fault, (b) relay BC for the B-C fault, and (c) relay CA for the C-A fault.

transformer. This reach puts the STATCOM within the fault loop if the relay has to operate. The ratio and phase-angle quantities for the phase relays are collected from the simulation online and fed to the fuzzy inference engine. The new reach, which should be observed beyond the infeed point, is calculated as described by (5). The transformer impedance as seen at the primary, $X1$ is added to (5) to obtain the total reach of the phase 21 relay. These computations are performed by a user-programmed FORTRAN block in PSCAD. The output reach given by this block is fed back to the adaptive mho circle in the simulation to form the closed-loop interaction. This block interacts with regular time intervals spaced by a user-defined time step. In the simulation considered here, the input ratio and phase-angle difference are fed to the block three times in a power frequency cycle. The effectiveness of the new relay is witnessed in Figs. 13 and 14. Fig. 13 plots the percentage error between the true reach to be observed by the three-phase relays and the corresponding reach values computed by the mechanism proposed. It can be noted that the difference in percentage error in case of the C-A fault is due to the dc offset which depends on the time instant at which the fault is initiated. The time instant of 15.0 s at which the fault is initiated will not correspond to the same point in the waveforms of the three-phase relay voltages.

The plot in Fig. 13 also shows how low the error is computed compared to that in Fig. 12. It can also be observed that there is a spike only very near the fault initiation period. But the adaptive logic adjusts very well to minimize the error to nearly zero during the overall fault duration (15 to 15.1 s in simulation time) from there onwards. The error in most of the fault duration is near zero. In fact, the relay can evidently be deemed to perform better in such fault conditions as seen in the plot. The error is lower than in the steady-state condition. Fig. 14 plots the trajectory of the impedance as seen by the three-phase relays (A-B, B-C, and C-A) with adapted zonal reaches. The circle which is innermost corresponds to the fixed or initial reach. The other two are the adaptive mho circles from the fuzzy scheme. The circle with the intermediary reach is the one which detects the fault, and the largest circle corresponds to the one when the fault clearance is detected. The fault is initiated at a time instant of 15.0 s and cleared at 15.1 s. Three points are marked on each diagram in the following order: the time instant before the fault is detected (15.015, 15.01, and 15.01 s for the three faults), the time instant when the fault is first detected (15.02 s in all cases), and the time instant when the fault is not detected because it is no more there (15.12, 15.12, and 15.11 s for the three cases). The fault is initiated at 15.0 s in all three cases. The first point which is pretty far away is, however, not shown for the purpose of clarity.

If the three plots are observed, the following can be deduced for all of the three phase-to-phase faults initiated at a simulation time of 15.0 s.

1) The trajectory of R-X points never enters the first circle, indicating a clear overreach with the infeed effect.
2) The time instant in which the fault is detected for the first time (15.02 s in all three cases) lies inside the intermediary circle thus validating that the second circle is the adaptive reach for that time instant. It can also be seen that it automatically lies inside the largest circle as well. However, this point is of no interest because the relay does not possess that characteristic at that point of time.

For simpler understanding, the illustrations in Fig. 14 show the original mho characteristics and only those two adaptive circles responsible for detecting the fault the first time and clearing the fault. The intermediary circles between these two time instants are also computed by the algorithm but not illustrated. Once the breaker is reclosed or the fault is cleared, the same routine is repeated.

Table I represents the maximum and minimum percentage errors in the reach seen by the traditional and fuzzy-based mho relays "in the fault duration span" and whether the phase faults are detected or not. It can be noted from Table I that the range of maximum and minimum percentage errors is far less in the fuzzy-based mho relay. In addition, the percentage errors in the fuzzy-based mho relay at the instant the fault is detected are 2.54%, 1.32%, and 2.79% for A-B, B-C, and C-A faults, respectively. At the same time instant, the percentage errors seen

TABLE I
PERCENTAGE ERROR IN THE PHASE RELAY REACH FOR PHASE-TO-PHASE FAULTS

Relay	Attribute	Phase Relay		
		A-B	B-C	C-A
Traditional Mho Circle	Max % Error	27.26	27.45	27.58
	Min % Error	1.52	1.49	1.50
	Fault Detected (Yes/No)	**No**	**No**	**No**
Proposed Fuzzy Scheme	Max % Error	4.11	4.06	6.58
	Min % Error	0.06	0.04	0.15
	Fault Detected (Yes/No)	**Yes**	**Yes**	**Yes**

TABLE II
PERCENTAGE ERROR IN PHASE RELAY REACH FOR DOUBLE-PHASE-TO-GROUND FAULTS

Relay	Attribute	Phase Relay		
		A-B	B-C	C-A
Traditional Mho Circle	Max % Error	27.66	27.81	30.53
	Min % Error	1.34	1.49	0.4
	Fault Detected (Yes/No)	**No**	**No**	**No**
Proposed Fuzzy Scheme	Max % Error	6.45	6.43	6.8
	Min % Error	0.07	0.009	0.004
	Fault Detected (Yes/No)	**Yes**	**Yes**	**Yes**

by the traditional mho relay, which do not detect the fault, are 18.46%, 19.40%, and 20.39%, respectively.

1) Double-Phase-to-Ground Faults: As mentioned earlier in Section II, the phase 21 relay does not generally cater to ground faults. However, its performance can always be measured for those ground faults involving more than one phase. Thus, Table II provides particulars for double-phase-to-ground faults, similar to those in Table I. The results indicate that the proposed methodology ensures that at least the phase relays work to expectation even when ground is involved.

Similar observations to those made from Table I apply to Table II. The relays never pick using the traditional mho while the adaptive mho picks up in all three cases. Further, the range of error is quite less when the fuzzy-based mho relay is applied. More important, the percentage errors in the reach observed by the adaptive phase relays A-B, B-C, and C-A, at the instant of fault detection, were 2.14%, 1.4%, and 1.95%, respectively The difference in percentage error can once again be attributed to the fact that the fault initiation instant (15.0 s) never corresponds to the same point on the waveforms of the three phases. The dc offset in the quantity measured by the secondary thus varies across three cases.

2) Three-Phase Fault: Since the three-phase fault involves all three phases and, thus, should enable all three-phase relays to trip, the adaptive mho diagram similar to the one depicted in Fig. 14 is adopted for illustration. The three overlapping circles in Fig. 15 also comprise the traditional mho (innermost), the adaptive mho which detects the fault (intermediary), and the adaptive mho which corresponds to fault clearance (outermost).

Fig. 15 depicts that all three-phase relays perform to expectation with the trajectory entering the second circle when the fault is first detected and exiting the outer circle when cleared. Moreover, the percentage errors in the reach observed by the adaptive phase relays A-B, B-C, and C-A, at the instant of fault detection, were 2.14%, 1.4%, and 1.95%, respectively.

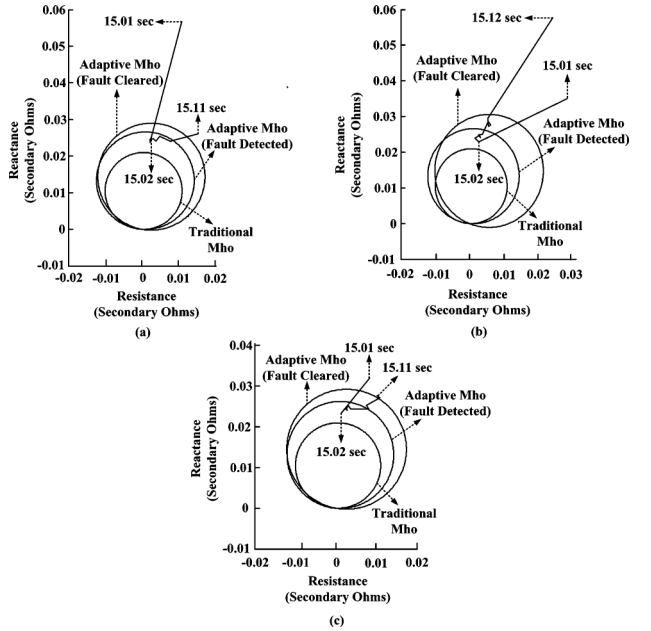

Fig. 15. Fuzzy adaptive mho zonal descriptions of (a) relay AB, (b) relay BC, and (c) relay CA for the three-phase fault.

D. Effect of Relay CT Saturation on the Phase 21 Function

The presence of asymmetrical current in the CT secondary due to dc offset has already been reported as an influencing factor in the previous section. Another factor which has the potential to create a much higher impact is the CT burden, which leads to saturation of the core. Saturation of the core would understandably result in a much lower secondary rms current than expected or desired, resulting in either a delay or failure of the relay to pick in worst cases. Both cases are accounted for in Fig. 16, effectively illustrating the effect of CT saturation. Per Fig. 16(a), the phase-to-phase fault A-B gets picked when the original relay CT burden of 0.5 Ω is modified to a value as large as 7.5 Ω. However, it is detected 0.02 s later than that shown in Fig. 14(a) even with the instant of fault initiation remaining the same (15.0 s). Fig. 16(a) comprises four circles among which the extra adaptive zone is the one named "adaptive mho II." It corresponds to the time instant of 15.04 s when the fault is detected. The effect of CT saturation is then studied with an even larger burden of 10 Ω in Fig. 16(b) which indicates that the fault goes unnoticed. Neither the intermediary circle "adaptive mho II" (supposed to have detected the fault) nor the outer circle "adaptive mho III" (supposed to have seen the fault cleared) picks any point on the trajectory.

E. Breaker Performance, Coordination, and Remote Closing

As pointed out in earlier sections, an intentional time delay is to be introduced for the phase 21 relay $R1$ shown in Fig. 17 in order to achieve coordination with the transmission-line relay. The breaker $B1$ is placed at the terminals of the generator. Breakers $B2$ and $B3$ represent the two breakers on the transmission line, which lies within the reach of the backup relay. Breaker $B1$ is tripped by the relay $R1$ after the specified delay if the breaker $B2$ does not trip due to failure. Once B1 trips, it issues a trip signal to B4 (as STATCOM reactive power support

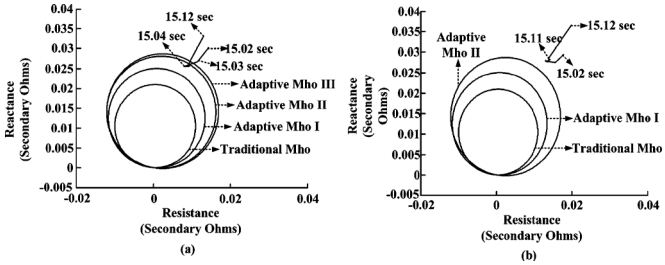

Fig. 16. Effect of elevating the CT burden to (a) 7.5 Ω and (b) 10 Ω on the adaptive mho relay performance during an A-B fault.

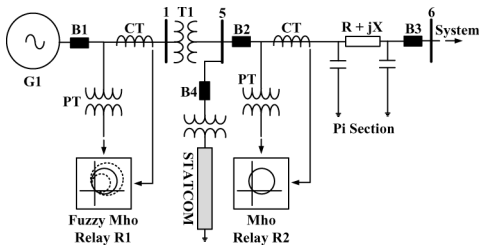

Fig. 17. Breaker arrangement for the method proposed.

is no longer needed for the generator) and remote-end breaker B3.

The simulated fault has less of a time duration at 0.1 s. For the sake of testing, the relay $R1$ is thus programmed to send the signal to breaker $B1$ after a time delay of 0.02 s. Breaker $B2$ is intentionally bypassed to imitate an error. For the AB fault introduced at the simulation time of 15 s, the relay $R1$ picks up at a simulation time of 15.02 s with the current and voltage transformers in place, as shown in Fig. 14(a). The breaker $B1$, however, issues the signal to trip only at 15.04 s, which is with the expected delay of 0.02 s specified. Once it trips, it issues signals to $B3$ (if required) and $B4$ to trip as well.

F. Effect of New Reach: Load Limitation

As explained in Section II, the generator capability has to be taken into consideration while deciding upon the reach. The reach should not limit generator loading so that a short-term disturbance, like a stable swing, enters the zonal reach of the relay. This point made becomes more significant when the solution adapts the relay reach with the help of fuzzy logic. The technique is robust based on the following text.

The relay reach incremented because the adjustment is only the equivalent value of the original reach fixed by (1). It is not an extra factor in the literal sense. The new reach is not a fixed value decided at one point in time and persisted with throughout to raise a concern for the load encroachment at some other point of time. Since the algorithm is run every few time steps, the modification in the relay reach is based on the system condition with infeed as of then and not at some point very far away. The concept of load encroachment would assume significance only if the technique utilized a predefined or fixed value regardless of current system conditions to correct the relay reach. However, the factor obtained from the FIS should not be seen as necessarily limiting the load since the load on the generator also changes with the infeed. Only the original values of $R2$ and $X2$ in (5) need to adequately cover for the GCC, which has already been taken care of by (1).

VI. Conclusion

This paper proposed a fuzzy-logic-based approach to address the effect of a STATCOM device installed within the relay reach of the phase 21 protection function. A couple of aspects making this work novel could be noted. First, the effect of current infeed was experimented on the generator backup protection. Literature has studied the effect of FACTS compensation or infeed only on the transmission-line distance relay reach so far. Second, the infeed was from the STATCOM, transiently varying in nature. This dynamic and flexible nature of the reactive compensation provided by STATCOM was an aspect very apt to being subjected to fuzzy-logic-based analysis given the capability of fuzzy logic to handle uncertainty with ease. Fuzzy logic employed in this paper exploited this fact and aimed to determine a compensating factor in an online fashion which, when applied to the existing mho circle, made it adaptive and enabled it to coordinate with the STATCOM control in a closed-loop simulation.

This paper could establish that while the presence of STATCOM could cause the conventional mho relay to maloperate in the case of each phase fault on the line chosen to be within the reach of the relay, the proposed adaptive fuzzy relay could issue the correct trip signals for the same. Effective simulations have also been carried out to illustrate the performance under miscellaneous conditions like CT saturation.

Appendix A
Machine and System Particulars

Synchronous Generators: 2 Q axis damper windings, 900 MVA, 20 kV (L-L), Inertia constant $H = 6.5$ (G1 and G2), 6.175 (G3 and G4), $R_a = 0.0025$ p.u., X_d =1.8 p.u., $X_q = 1.7$ p.u., $X'_d = 0.3$ p.u., $X'_q = 0.55$ p.u., $X''_d = 0.25$ p.u., $X''_q = 0.25$ p.u., $T'_{d0} = 8$ s, $T'_{q0} = 0.4$ s, $T''_{d0} = 0.03$ s, $T''_{q0} = 0.05$ s. Initial conditions: terminal voltage $V = 1.03$ p.u. (G1 and G3), 1.01 p.u. (G2 and G4).

Generator Stepup Transformer: two-winding transformer: 900 MVA, 20 kV/230 kV, $X_1 = 0.15$ p.u.

Transmission Line: 230 kV (L-L), 100 MVA, $R = 0.053$ Ω/km, $X = 0.53$ Ω/km for all lines except line 5-6. Line 5-6, which is being protected by the relay, is modeled as a pi section. Line 5-6: 25 km, $R = 0.00005$ p.u./km, $X = 0.0005$ p.u./km, $B = 0$ p.u./km, zero-sequence compensation factor $(Z_0/Z_1) = 1.5$.

Exciter: IEEE ST1A type, $T_r = 0.01$ s, $T_C = 1.0$ s, $T_B = 10.0$ s, ILR = 4.4 p.u., KLR = 4.54 p.u., $VR_{\mathrm{MAX}} = 6.43$ p.u., VR_{MIN} = -6.0 p.u., $K_C = 0.038$ p.u., $K_A = 50$ p.u.

Power System Stabilizer: (IEEE PSS1A) Washout Time Constant $T_w = 1$ s, $T_1 = T_3 = 0.14714$ s, $T_2 = T_4 = 0.17643$, $K_1 = K_2 = 0.54714$.

Thermal Governor: GE Mechanical-Hydraulic controls, permanent droop $R = 0.05$ p.u., speed relay time constant TSR = 0.1 p.u., Gate Servo Time Constant TSM = 0.2 p.u.

Thermal Turbine: IEEE type 2 thermal turbine $K_1 = K_3 = K_5 = K_7 = K_2 = K_4 = K_6 = K_8 = 0.125$ p.u., $T_4 = T_5 = T_6 = T_7 = 1$ s.

APPENDIX B
STATCOM PARTICULARS

Coupling Transformer: shunt-connected, three-phase, two-winding Y-Δ transformer: 100 MVA, 230 kV/20 kV, positive-sequence leakage reactance $X_1 = 0.1$ p.u.

Converter: two-level, three-phase, six pulse voltage-source converter: 15 mF DC link capacitor, pulse width modulation based firing scheme.

DC Control (Fig. 5): $G = 0.2, T_1 = 0.01$ s, $T_2 = 0.4$ s.

AC Control (Fig. 5): $G = 1, T_1 = 0.02$ s, proportional gain $P = 10$, integral gain $I = 0.01$.

REFERENCES

[1] J. M. Gers and E. J. Holmes, *Protection of Electrical Distribution Networks, Power and Energy Series 47*, 2nd ed. London, U.K.: Inst. Eng. Technol. (IET), 2005, ch. 9.

[2] J. L. Blackburn and T. J. Domin, *Protective Relaying Principles and Applications*, 3rd ed. New York: Taylor & Francis, 2007, ch. 2.

[3] S. J. Horowitz and A. G. Phadke, *Power System Relaying*, 3rd ed. Hoboken, NJ: Wiley, 2008, ch. 5.

[4] K. E. Arroudi, G. Joos, and D. T. McGillis, "Operation of impedance protection relays with the STATCOM," *IEEE Trans. Power Del.*, vol. 17, no. 2, pp. 381–387, Apr. 2002.

[5] T. S. Sidhu, R. K. Varma, P. K. Gangadharan, F. A. Albasri, and G. R. Ortiz, "Performance of distance relays on shunt-FACTS compensated transmission lines," *IEEE Trans. Power Del.*, vol. 20, no. 3, pp. 1837–1845, Jul. 2005.

[6] F. A. Albasri, T. S. Sidhu, and R. K. Varma, "Performance comparison of distance protection schemes for shunt-FACTS compensated transmission lines," *IEEE Trans. Power Del.*, vol. 22, no. 4, pp. 2116–2125, Oct. 2007.

[7] P. K. Dash, A. K. Pradhan, G. Panda, and A. C. Liew, "Digital protection of power transmission lines in the presence of series connected FACTS devices," in *Proc. IEEE Power Eng. Soc. Winter Meeting*, Jan. 23–27, 2000, vol. 3, pp. 1967–1972.

[8] J. V. V. N. Bapiraju, J. U. Shenoy, K. G. Sheshadri, H. P. Khincha, and D. Thukaram, "Implementation of DSP based relaying with particular reference to effect of STATCOM on transmission line protection," in *Proc. Int. Conf. Power Syst. Technol.*, Nov. 21–24, 2004, vol. 2, pp. 1381–1385.

[9] M. J. Charles and Working group J-5 of the rotating machinery subcommittee, Power System Relay Committee, "Coordination of generator protection with generator excitation control and generator capability," in *Proc. IEEE Power Eng. Soc. Gen. Meeting*, Jun. 24–28, 2007, pp. 1–17, .

[10] *IEEE Guide for AC Generator Protection*, IEEE Standard C37.102-1995, 1996.

[11] "A survey of generator back-up protection practices," *IEEE Trans. Power Del.*, vol. 5, no. 2, pp. 575–584, Apr. 1990.

[12] D. Reimert, *Protective Relaying for Power Generation Systems*. Boca Raton, FL: CRC, 2006, ch. 4.

[13] J. S. Dudor and L. K. Padden, "Protective relay application for generators and transformer," *IEEE Ind. Appl. Mag.*, vol. 3, no. 4, pp. 22–35, Jul./Aug. 1997.

[14] B. Ravikumar, D. Thukaram, and H. P. Khincha, "An approach using support vector machines for distance relay coordination in transmission system," *IEEE Trans. Power Del.*, vol. 24, no. 1, pp. 79–88, Jan. 2009.

[15] K. K. Li, L. L. Lai, and A. K. David, "Stand alone intelligent digital distance relay," *IEEE Trans. Power Syst.*, vol. 15, no. 1, pp. 137–142, Feb. 2000.

[16] H. Rastegar and A. P. Khansaryan, "A new method for adaptive distance relay setting in the presence of SSSC using neural networks," in *Proc. 1st IEEE Conf. Ind. Electron. Appl.*, May 24–26, 2006, pp. 1–8.

[17] B. Das and J. V. Reddy, "Fuzzy-logic-based fault classification scheme for digital distance protection," *IEEE Trans. Power Del.*, vol. 20, no. 2, pt. 1, pp. 609–616, Apr. 2005.

[18] K. Razi, M. T. Hagh, and G. Ahrabian, "High accurate fault classification of power transmission lines using fuzzy logic," in *Proc. Int. Power Eng. Conf.*, Dec. 3–6, 2007, pp. 42–46.

[19] *PSCAD/EMTDC User's Guide*. Winnipeg, MB, Canada: Manitoba HVDC Res. Ctr., 2005.

[20] P. Kundur, *Power System Stability and Control*. New York: McGraw-Hill, 1994, ch. 12.

[21] *IEEE Recommended Practice for Excitation System Models for Power System Stability Studies*, IEEE Standard 421.5-2005 (Rev. IEEE Standard 421.5-1992), 2006.

[22] A. M. Gole, S. Filizadeh, R. W. Menzies, and P. L. Wilson, "Optimization-enabled electromagnetic transient simulation," *IEEE Trans. Power Del.*, vol. 20, no. 1, pp. 512–518, Jan. 2005.

[23] N. G. Hingorani and L. Gyugyi, *Understanding FACTS: Concepts and Technology of Flexible AC Transmission Systems*. New York: IEEE Press, 2000.

[24] J. R. Timothy, *Fuzzy Logic With Engineering Applications*, 3rd ed. Hoboken, NJ: Wiley, 2010, ch. 4.

Sivaramakrishnan Raman received the B.Tech. degree in electrical and electronics engineering from SASTRA University, Thanjavur, India, in 2008 and the Master's degree in IT in power systems from International Institute of Information Technology, Hyderabad, India, in 2012.

He was an exchange student at the Power Systems Research Laboratory, University of Saskatchewan, Saskatoon, SK, Canada, during 2011. Currently, he is with GE-Energy, Hyderabadchnology Center, India. His research interests include power systems protection and control, and smart grids.

Ramakrishna Gokaraju (S'88–M'00) received the M.Sc. and Ph.D. degrees in electrical and computer engineering from the University of Calgary, Calgary, AB, Canada, in 1996 and 2000, respectively.

He joined the University of Saskatchewan, Saskatoon, SK, Canada, in 2003 and is currently an Associate Professor. From 1992 to 1994, he was a Graduate Engineer with Larsen & Toubro-ECC, Madras, India, and a Research Associate with the Indian Institute of Technology, Kanpur, India. During 1999–2002, he was a Research Scientist with the Alberta Research Council, Canada, and a Staff Software Engineer with IBM Toronto Lab, Canada. His research interests include power systems protection and control, and smart grids.

Amit Jain (M'05) received the M.Sc. and Ph.D. degrees in electrical engineering from the Indian Institute of Technology, Delhi, India.

He was with ALSTOM on the power supervisory control and data-acquisition systems and later on he was a Postdoctoral Researcher in Japan and South Korea. He joined the International Institute of Information Technology, Hyderabad (IIIT H), India, in 2007 and is currently a Research Assistant Professor in the Power Systems Research Center. His research interests are power systems real-time monitoring and control, phasor measurement unit, power systems planning and economics, and artificial-intelligence applications.